Geotech Geol Eng (2022) 40:1043–1060
https://doi.org/10.1007/s10706-021-01941-6

ORIGINAL PAPER

# A New SPT-Based Method for Estimating Axial Capacity of Driven Piles in Glacial Deposits

**Markus Jesswein · Jinyuan Liu**

Received: 11 May 2020 / Accepted: 9 July 2021 / Published online: 1 September 2021


**Abstract** This paper proposes a new design method for the axial capacity of driven piles in glacial deposits with the standard penetration test (SPT) based on a database of 53 full-scale pile load tests. These static load tests were conducted on driven steel H and pipe piles in glacial deposits across the province of Ontario, Canada. The piles were tested in either compression and/or tension to plunging failures and had sufficient soil measurements, in particular SPT measurements, along their length for further analyses. The SPT is the most popular, and in many cases the only, field exploration technique applied in Ontario for gravel or cobble rich glacial deposits. First, the performance of existing SPT-based design methods was evaluated with the results from these pile load tests. On average, the existing design methods overestimated the measured capacity by a factor of 1.62 with a coefficient of variation (COV) of 58%. Second, a new design method was proposed according to the effective stress method to better correlate side and tip resistances with the SPT blow count (N-value). The new design method considers both the pile type and soil gradation. A set of pile load tests collected from literature were applied to validate the newly proposed method. It was found that the newly proposed design method can provide an unbiased prediction with a significantly reduced variation.

M. Jesswein
Department of Civil Engineering, Ryerson University, Toronto, ON, Canada
e-mail: markus.jesswein@ryerson.ca

J. Liu (✉)
Department of Civil Engineering, Ryerson University, 350 Victoria St, Toronto, ON M5B 2K3, Canada
e-mail: jinyuan.liu@ryerson.ca

**Keywords** Driven piles · Ultimate axial capacity · Prediction methods · Standard penetration test · Glacial deposits

## List of Symbols

| | |
|---|---|
| $A$ | Coefficient to calculate the unit side resistance |
| $a$ | Coefficient to calculate the unit side resistance from Aoki and Velloso (1975) |
| $A_p$ | Cross-sectional area at the tip of a pile |
| $A_s$ | Side area of a pile |
| $B$ | Coefficient to calculate the unit side resistance |
| COV | Coefficient of variation |
| $C_F$ | Empirical correction factor |
| $Cu$ | Undrained shear strength |
| $D$ | Diameter or width of pile |
| $i$ | Individual layer in cohesive soil |
| $j$ | Individual layer in cohesionless soil |
| $K$ | Coefficient to calculate the unit tip resistance |
| $K_\delta$ | Coefficient of lateral earth pressure |
| $L$ | Pile embedment length |
| $L/D$ | Slenderness ratio of the pile |
| $N$ | Blow count, or N-value, from standard penetration test (SPT) |
| $\overline{N}$ | Average SPT N-value along a pile |

| | |
|---|---|
| $n$ | Number of piles, tests, or the sample size |
| $N_c$ | End bearing factor for cohesion |
| $N_{cor}$ | Corrected SPT N-value for 60% hammer efficiency ($N_{60}$ for cohesive soils and $(N_1)_{60}$ for cohesionless soils) |
| $\overline{N}_{cor}$ | Average corrected SPT N-value along the side of a pile |
| $N_f$ | SPT N-value from the field |
| $N_p$ | SPT N-value at the pile tip |
| $N_q$ | End bearing factor for friction |
| $P$ | Perimeter of a pile |
| $Pa$ | Atmospheric pressure (100 kPa) |
| $PI$ | Plasticity index |
| $Qp$ | Pile tip resistance |
| $q_p$ | Unit tip resistance of a pile |
| $Qs$ | Pile side resistance |
| $q_s$ | Unit side resistance of a pile |
| $Qu$ | Ultimate pile capacity |
| $Qu_p$ | Predicted ultimate capacity of a pile |
| $R^2$ | Coefficient of determination |
| $T$ | Total number of soil types or categories |
| $\alpha$ | Empirical adhesion factor |
| $\alpha_t$ | End bearing correction factor |
| $\beta$ | Empirical adhesion factor |
| $\delta$ | Soil-pile interface friction angle |
| $\phi'$ | Soil friction angle |
| $\sigma'$ | Effective stress |
| $\sigma_t'$ | Effective stress at the pile tip |

## 1 Introduction

Pile foundations are commonly designed to support bridges and buildings in weak soils, but accurately predicting the capacity of a pile is still a challenge due to many influential factors, such as the pile type, pile geometry, and installation method. In particular, ground conditions provide additional uncertainties for the prediction. For example, glacial deposits, commonly found in the province of Ontario, Canada, are well known for their inconsistent material properties (Barnett 1992; Legget 1965; Milligan 1976), and it is extremely challenging for practice engineers to accurately characterize their heterogeneous properties. In addition, a limited number of site investigation techniques are available for glacial deposits due to their generally dense or very stiff conditions and gravel and/or cobble bearing characteristics. The standard penetration test (SPT) is the most popular, and in many cases the only, site investigation method in Ontario for this kind of ground.

Over the last few decades, several approaches were proposed to predict the ultimate capacity of a pile with SPT blow counts (N-values) (Alkroosh and Nikraz 2014; Aoki and Velloso 1975; Benali et al. 2017; Brown 2001; Decourt 1982, 1995; Martin et al. 1987; Meyerhof 1956, 1976; Nordlund 1963, 1979; Shariatmadari et al. 2008; Shioi and Fukui 1982; Thorburn and MacVicar 1971; Xiao and Yang 2011; Zhang and Chen 2012). These approaches can be classified into direct or indirect design methods. Direct methods correlate directly the SPT N-value to the pile resistance. These methods are typically developed for either cohesive or cohesionless soils, but these two idealized soil types cannot accurately consider glacial deposits with a large range of unsorted grain sizes. Based on a database of 98 piles, Briaud and Tucker (1988) discovered the direct SPT method proposed by Meyerhof (1956, 1976) over predicted the capacity by a factor of 1.73 on average with a coefficient of variation (COV) of 72% for the ratio between the predicted to measured capacity ($Qu_p/Qu_m$). Indirect design methods first correlate the SPT N-values to the soil strength parameters, namely the friction angle and undrained shear strength, and then apply the shear strength parameters for the capacity prediction. Compared to direct approaches, these methods can offer more consistent predictions as they rely on soil mechanic theories to determine the pile resistance. However, variabilities still exist as empirical judgement is required to correlate SPT N-values with the shear strength of soils. For a reliability analysis on H piles in layered soils, Tang and Phoon (2018) obtained a $Qu_p/Qu_m$ that ranged from 0.44 to 2.5 with predictions by the American Petroleum Institute (API) (2000) $\alpha$ and Nordlund (1963, 1979) $\beta$ methods using SPT N-values. The variability in design can be contributed to the quality of the SPT results, which depends on the ground condition; drilling method; efficiency of the hammer energy delivered to the head of the drill rod; and dynamic behavior of applying the blow counts (Yagiz et al., 2008).

Due to the challenges and uncertainties in design and ground conditions, pile load tests have been commonly used to verify design assumptions in practice and to develop design methods for local soil conditions (Briaud and Tucker 1988; Brown 2001; Golafzani et al. 2020; McVay et al. 2000; Tang and Phoon 2018). A total of 53 pile load tests were selected from a database collected by the Ministry of Transportation of Ontario (MTO) from 1954 to 1992. This study evaluates the performance of existing design methods with these piles and then proposes a new SPT-based design method for driven piles in glacial deposits. In order to offer improvements for the prediction of the pile capacity, the new design method considers various soil compositions that are unique characteristics of glacial deposits. In addition, the new method also applied an effective stress approach for the pile resistance.

## 2 Existing Design Methods for the Axial Capacity of Piles

The ultimate axial capacity ($Qu$) of a compression pile can be simplified into two components: the side resistance ($Qs$) along the pile and the tip resistance ($Qp$).

$$Qu = Qs + Qp = q_s A_s + q_p A_p \tag{1}$$

where $q_s$ is the unit side resistance, $q_p$ is the unit tip resistance, and $A_s$ and $A_p$ are respectively the side surface area and tip area of the pile.

Over the decades, many methods have been developed or proposed to estimate $q_p$ and $q_s$, including the direct SPT approach (Meyerhof 1976), $\alpha$ method (Tomlinson 1957), and $\beta$ method (Burland 1973).

Empirical correlations were proposed by many researchers to directly correlate $q_s$ and $q_p$ with SPT N-values (Alkroosh and Nikraz 2014; Aoki and Velloso 1975; Benali et al. 2017; Brown 2001; Decourt 1982, 1995; Martin et al. 1987; Meyerhof 1956, 1976; Shariatmadari et al. 2008; Shioi and Fukui 1982; Thorburn and MacVicar 1971; Xiao and Yang 2011; Zhang and Chen 2012). Generally, the correlations assume the pile resistances are linearly proportionate to the measured N-value:

$$q_s = A\overline{N} + B \tag{2}$$

$$q_p = KN_p \tag{3}$$

where $\overline{N}$ is the average SPT N-value, which is commonly calculated as the arithmetic average along the pile length; $N_p$ is the SPT N-value at the pile base; and $A$, $B$, and $K$ are coefficients. The coefficients in Eqs. (2) and (3) were found by fitting with trial-and-error (Aoki and Velloso 1975) or by regressing the SPT N-values to pile resistances (Brown 2001). These empirical correlations differ on the soil conditions as shown in Table 1 for $q_s$ and Table 2 for $q_p$. Coefficient $A$ is influenced by the cohesion of a soil and is generally lower for sandy soils compared to clayey soils, but the opposite trend occurs for Coefficient $K$ as sandy soils are generally less compressible and have a higher $Qp$. Since cohesive soils are more influenced by stress history, plasticity, and compressibility, empirical methods are more popular with cohesionless soils. Some references proposed a single value for Coefficient $A$ or $K$ for both cohesive and cohesionless soils, but their design methods are likely limited to the regional soil conditions, such as Brown (2001) and Decourt (1982). On the other hand, Aoki and Velloso (1975) considers many different soil types and provides a wide range of coefficients for $Qs$ and $Qp$ to achieve better predictions.

For cohesive soils, $\alpha$ methods are commonly applied to assess the pile capacity during short-term and have the following expressions with the undrained shear strength ($Cu$):

$$q_s = \alpha Cu \tag{4}$$

$$q_p = N_c Cu \tag{5}$$

where $\alpha$ and $N_c$ are an empirical adhesion and end bearing factor, respectively. A value of 9 may be used for $N_c$ (Meyerhof 1976). Direct and indirect methods for cohesive soils can be very similar mathematically as most empirical methods linearly correlate $Cu$ to SPT N-values (Kulhawy and Mayne 1990; Sivrikaya and Toğrol 2006; Sowers 1951). Unfortunately, correlations between $Cu$ and N-values are usually poor. First, the measured $Cu$ can vary depending on the strain rate and direction of shear applied by a testing technique (Jardine et al. 2005). Next, most correlations do not consider the influence of effective stress or soil confinement and were developed with unconsolidated undrained (UU) triaxial and/or unconfined compressive strength (UCS) tests (Kulhawy and Mayne 1990). Greater confinement will likely lead to a larger side

**Table 1** Existing Correlation Methods for SPT N-values and Unit Side Resistance ($q_s$)

| Soil type | References | Equation for $q_s$ (kPa) | Remarks |
|---|---|---|---|
| Cohesive | Shioi and Fukui (1982) | $q_s = 9.8\overline{N}$ | |
| Cohesionless | Meyerhof (1976) | Large displacement piles: | |
| | | $q_s = 1.9\overline{N} \leq 100$ | |
| | | Low Displacement Piles: | |
| | | $q_s = 1.0\overline{N} \leq 100$ | |
| | Shariatmadari et al. (2008) | $q_s = 3.65\overline{N}$ | For this reference, $\overline{N}$ is the geometric average |
| | Shioi and Fukui (1982) | $q_s = 1.9\overline{N}$ | |
| | Thorburn and MacVicar (1971) | Silts: $q_s = 1.6\overline{N}$ | |
| Cohesive to cohesionless | Aoki and Velloso (1975) | $q_s = Aa\overline{N}$ | For driven piles, $A$ varies by soil type and ranges from 56 for clays to 280 for sands; $a$ is an empirical coefficient and ranges from 0.012 for medium sands to 0.04 for clays |
| | Brown (2001) | $q_s = 1.8\overline{N} + 25$ | $3 \leq N \leq 50$ |
| | Decourt (1982) | $q_s = 3.3\overline{N} + 9.8 \leq 170$ | $3 \leq N \leq 50$ |
| | Decourt (1995) | $q_s = 2.8\overline{N} + 9.8$ | |

**Table 2** Existing correlation methods for SPT N-values and Unit Tip Resistance ($q_p$)

| Soil type | References | Equation for $q_p$ (kPa) | Remarks |
|---|---|---|---|
| Cohesive | Decourt (1982) | $q_p = 118N_p$ | $3 \leq N_p \leq 50$ |
| | Decourt (1995) | Clay: $q_p = 100N_p$ | |
| | | Clayey Silt: $q_p = 165N_p$ | |
| | Martin et al. (1987) | $q_p = 192N_p$ | |
| Cohesionless | Decourt (1982) | $q_p = 392N_p$ | |
| | Decourt (1995) | Sandy Silt: $q_p = 205N_p$ | |
| | | Sand: $q_p = 325N_p$ | |
| | Martin et al. (1987) | Silt/Sandy Silt: $q_p = 335N_p$ | |
| | | Sand: $q_p = 431N_p$ | |
| | Meyerhof (1976) | $q_p = 38(L/D)N_p \leq 383N_p$ | |
| | Shariatmadari et al. (2008) | $q_p = 385N_p$ | |
| | Thorburn and MacVicar (1971) | Glacial Till and Silt: | |
| | | $q_p = 239N_p$ | |
| Cohesive to cohesionless | Aoki and Velloso (1975) | $q_p = KN_p$ | For driven piles, $K$ varies by soil type and ranges from 112 for clays to 560 for sands |
| | Brown (2001) | $q_p = 170N_p$ | $3 \leq N_p \leq 50$ |
| | Shioi and Fukui (1982) | If $L/D \geq 5$, $q_p = 287N_p$ | $L/D$ is the slenderness ratio, where $D$ is the pile diameter or width |
| | | If $L/D < 5$ (solid piles), | |
| | | $q_p = (100 + 40L/D)N_p$ | |

resistance. In addition, especially for sensitive soils, the dynamic nature of a SPT generates excess pore pressures, which reduces the effective stress and results in low N-values (Jardine et al. 2005).

For cohesionless soils and the long-term conditions of cohesive soils, direct methods and some $\alpha$ methods are stress independent and lack consideration for the overburden stress that contributes to the lateral confinement of soil on the pile; thus, the effective stress methods may be preferred for design, also applied in this study. According to an American survey by AbdelSalam et al. (2012), one popular approach is the effective stress method proposed by Nordlund (1963, 1979). Effective stress or $\beta$ methods have the general forms:

$$q_s = \beta\sigma' \tag{6}$$

$$q_p = N_q\sigma'_t \tag{7}$$

where $\beta$ is an adhesion coefficient, $N_q$ is an end bearing coefficient, $\sigma'$ is the effective stress along a pile, and $\sigma_t'$ is the effective stress at the pile tip. Since $\beta$ and $N_q$ are proportionate to the soil friction angle ($\phi'$), this study will assume the SPT N-value is also proportionate to these parameters while using the effective stress approach. In this paper, $N_q$ is back-calculated with the measured unit tip resistance and vertical effective stress at the pile tip, $\sigma_t$'. $N_q$ is expressed as a function of the SPT N-value. It is assumed that excess pore pressures have sufficiently dissipated during the pile load tests also the effects of set-up, the regaining of soil strength with time, is ignored in this study. These assumptions are considered reasonable since in most cases the soil layers are alternating and silts are commonly found in most layers. In summary, there are plenty of drainage paths available along the piles.

Several references (Kolk and Van der Velde 1996; Meyerhof 1976; Shioi and Fukui 1982; Van Dijk and Kolk 2011) experienced varying impacts with the pile length. For example, Meyerhof (1976) recommends limiting the side resistance once a particular, or critical, depth is reached, but Fellenius (2019) suggests the appearance of a maximum side resistance is likely due to the accumulation of residual loads towards a pile base. A pile can experience residual loads along its length even though axial loads are not applied to its head. Among several reasons, residual loads develop from consolidating soil that generate a negative side resistance along a pile as excess pore pressures dissipate after pile driving (Fellenius 2019). It is difficult, however, to quantify the residual loads in non-instrumented piles (Fellenius 2019). In this paper, the side resistance will not be limited and will be assumed to be proportionate to the effective stress and soil strength.

## 3 Studied Pile Load Test Database From MTO

### 3.1 Pile Load Test Database

Pile load tests used in this study were located in various regions of Ontario, as shown in Fig. 1. The pile widths varied within a narrow range from 299 to 324 mm, relatively small, due to the local contractor preference and difficulty of driving a large size pile in dense or stiff glacial deposits. The pile lengths ranged from 3 to 45 m, but most were from 12 to 25 m. Most sites had heterogeneous ground profiles. For example, Site 33 near Buttonville had intermittent layers of clayey silts and silty sands, and Fig. 2a and b shows the varying gravel content and SPT N-values measured at Site 38 near Peterborough. Although soft and loose soils were found in some sites, most of the cohesionless soils were compact to very dense, while cohesive soils were usually classified as firm to very stiff. In all, a variety of soil conditions were encountered in the studied sites. Figure 2c shows the load-settlement curves of two steel pipe piles (P4 and P5) at the site along with the identified failure loads. The dimensions of these piles are shown below the load-settlement curve figure.

### 3.2 Pile Load Test Procedures

In this study, the focus was on driven piles subjected to standard (slow) maintained-static compression and/or tension tests. The axial loads were applied to the top of the piles by hydraulic jacks that acted against an anchored reaction frame, weighted box, or weighted platform. Loads were increased until failure occurred in increments equal to 25% of the estimated design load. For each increment, the load remained constant until the rate of settlement became less than 0.25 mm per hour or until a 2 h duration was reached (MTO 1993). Based on these criteria, the time interval between load increments may have varied slightly

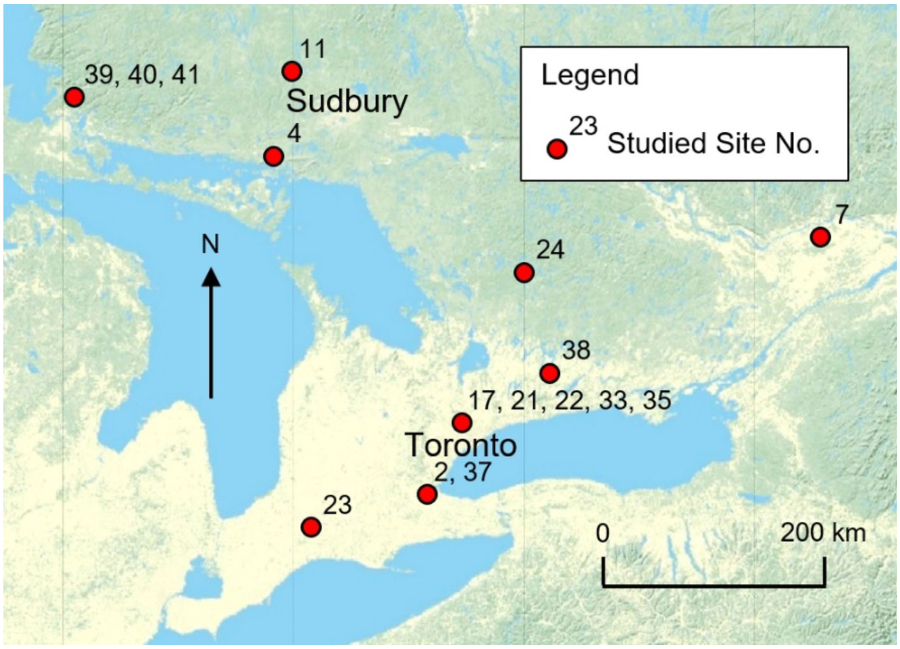


**Fig. 1** Locations of Studied Sites in Ontario, Canada

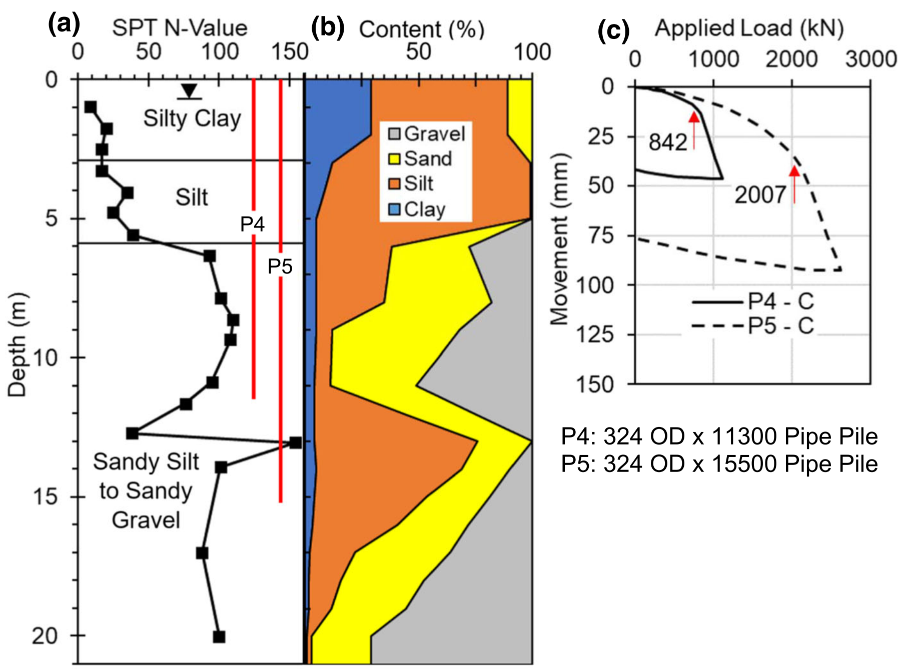


**Fig. 2** Example of the **a** Field SPT N-values, **b** Soil contents, and **c** Load–displacement response of piles at site 38

under 2 h. Unloading was conducted with the same increment as the loading stages (MTO 1993). The pile displacement was taken as the average reading of the four gauges mounted on the top of the pile (MTO 1993). As examples, Fig. 2c shows load–displacement curves from two piles at Site 38.

A majority of the piles were tested with both compression and extension load tests. The compressive load test was typically performed first, and the set-up time between installation and testing varied from a week to a month. A short set-up time was selected for piles in mainly cohesionless soils, while a longer set-up time for piles in cohesive soils.

### 3.3 Selected Cases for this Study

Among the pile load tests in the database, the piles were selected for this study based on the following conditions: plunging failure; sufficient geotechnical information; non-organic ground; and steel driven piles. Also, sensitive cohesive soils were not encountered in the selected pile cases. In the end, a total of 32 piles (16 H and 16 steel pipe) were selected for this study, where 21 piles were subjected to both tensile and compressive tests; 9 piles were only subjected to compression loads; and 2 piles were only tested with tension loads. All the pipe piles were capped and filled with concrete before driving, except two open-ended ones. The details of the pile geometry and site conditions and pile load test data are shown in Table 3.

### 3.4 Resistances Interpreted from Pile Load Tests

Many different methods exist to identify the pile capacity from the load–displacement curve. The identified capacity value ($Qu_m$) varies depending on the selected method, which will slightly influence the remaining analysis. Although the Davisson Offset Method is the most popular one, it is an empirical method and may inaccurately estimate the yielding point (Fellenius 1980). Since the tested piles in this study achieved the plunging failure or experienced a significant amount of displacement, the yielding loads for this investigation were evaluated with the De Beer method, which identifies the pile capacity as the load at the intersection of two slopes from the load–displacement curve plotted in a double-log scale (De Beer 1967, 1968).

For the piles subjected to both compression (conducted first) and tension tests, it was assumed that the tension capacity ($Qs$), identified from the tension test curve, was equivalent to the skin resistance component during the compression test. A similar approach was applied by Boonstra (1936). Then, $Qp$ was assumed to be the difference between $Qs$ and the compression capacity $Qu$ identified from the compression curve.

### 3.5 Soil Conditions

Soil conditions were provided by borehole logs, but every site varied greatly in the extent and diversity of the field and laboratory tests. A variety of soil measurements were collected for each site, but most the results were from SPT and Atterberg limits. In general, measurements from the database included liquidity indices; plasticity indices; natural moisture contents; unit weights; and compositions of gravel, sand, silt, and clay; and soil classification according to the grain-size distribution. Soil classifications and SPT N-values were commonly recorded at different depths.

With the recommendations from Canadian Geotechnical Society (CGS) (2006), the field N-values ($N_f$) were corrected to $N_{60}$ for 60% hammer efficiency in cohesive soils and to $(N_1)_{60}$ with an additional overburden pressure correction ($C_n$) in cohesionless soils:

$$N_{60} = N_f \cdot C_s \cdot C_b \cdot C_r \cdot E_H \tag{8}$$

$$(N_1)_{60} = C_n \cdot N_{60} \tag{9}$$

where

$$C_n = 0.77 \log_{10}\left(\frac{1920}{\sigma'}\right) \leq 1.5 \tag{10}$$

A few assumptions were taken for all cases for the correction, including a hammer efficiency ($E_H$) of 0.75 for a donut hammer type with an estimated rod energy ratio of 45%; a sampling correction factor ($C_s$) of 1 for a standard sampler; and a borehole correction factor ($C_b$) of 1 for a borehole diameter of approximately 100 mm. The rod length correction factor ($C_r$) ranges from 0.75 to 1 depending on the depth of the sample. These assumptions will slightly influence the results of the analysis.

### 3.6 Influence of Gravel Content

Gravels were commonly encountered in glacial deposits in Ontario, especially within the cohesionless soils. Figure 3 shows the variability of the corrected N-value ($N_{cor}$) with boxplots and the influence of the gravel content. In the figure, $n$ is the number of

**Table 3** Summary of pile geometry, soil condition, and load test results on the selected piles

| Case no | Site no | Pile no | Pile type[a] | Length[b](m) | Embedded soil type[c] | *Qu* (kN) | *Qs* (kN) | *Qp* (kN) | Notes |
|---|---|---|---|---|---|---|---|---|---|
| 1 | 2 | 5 | 305 OD Pipe | 5.85 | Sand | 812 | | | Open-ended |
| 2 | 4 | 2 | 324 OD Pipe | 35.94 | Silt and clayey silt | 553 | | | 343 mm ∅ shoe |
| 3 | 7 | 2 | HP 310 × 79 | 21.70 | Clay and silty sand | 827 | | | |
| 4 | 11 | 1 | HP 310 × 79 | 26.82 | Sand to silt | 550 | | | |
| 5 | 17 | 2 | HP 310 × 110 | 26.47 | Clayey silt to sand | 2482 | | | |
| 6 | 22 | 3 | 324 OD Pipe | 15.30 | Clayey silt | 163 | 148 | 15 | 343 mm ∅ shoe |
| 7 | 22 | 4 | 324 OD Pipe | 30.15 | Clayey Silt | 937 | | | 343 mm ∅ shoe |
| 8 | 23 | 2 | 324 OD Pipe | 3.02 | Silty clay | 442 | 217 | 225 | 343 mm ∅ shoe |
| 9 | 23 | 3 | HP 310 × 110 | 3.05 | Silty clay | 425 | 255 | 170 | |
| 10 | 24 | 2 | 324 OD Pipe | 15.39 | Sand | 608 | 402 | 206 | 343 mm ∅ shoe |
| 11 | 24 | 3 | 324 OD Pipe | 22.40 | Sand | 667 | 443 | 224 | 343 mm ∅ shoe |
| 12 | 24 | 4 | HP 310 × 79 | 22.40 | Sand | 1371 | 420 | 951 | |
| 13 | 24 | 5 | HP 310 × 79 | 15.39 | Sand | 702 | 275 | 427 | |
| 14 | 28 | 2 | HP 310 × 79 | 18.29 | Clayey silt | 471 | 331 | 141 | |
| 15 | 28 | 7 | 324 OD Pipe | 6.10 | Clayey silt | 658 | 569 | 89 | 343 mm ∅ shoe |
| 16 | 28 | 8 | 324 OD Pipe | 18.29 | Clayey silt | 659 | 442 | 217 | 343 mm ∅ shoe |
| 17 | 33 | 2 | 324 OD Pipe | 32.95 | Clayey silt and silty sand | 2095 | | | 342 mm ∅ shoe |
| 18 | 35 | 1 | HP 310 × 110 | 14.69 | Layered clayey silt and silty sand | 1592 | 523 | 1069 | |
| 19 | 35 | 4 | 324 OD Pipe | 14.69 | Layered clayey silt and silty sand | 1507 | 759 | 748 | 343 mm ∅ shoe |
| 20 | 35 | 5 | HP 310 × 110 | 27.58 | Layered clayey silt and silty sand | 2714 | 1524 | 1190 | |
| 21 | 37 | 3 | HP 310 × 79 | 14.48 | Sand to silty sand | 1042 | 345 | 700 | |
| 22 | 37 | 5 | HP 310 × 79 | 31.24 | Sand to sandy silt | 1609 | 444 | 1165 | |
| 23 | 37 | 6 | HP 310 × 110 | 14.48 | Sand to silty sand | 717 | 413 | 304 | |
| 24 | 37 | 8 | HP 310 × 110 | 30.92 | Sand to silty sand | 1566 | 699 | 867 | |
| 25 | 38 | 4 | 324 OD Pipe | 11.30 | Silty clay and silt to silty sand | 842 | | | Open-ended |
| 26 | 38 | 5 | 324 OD Pipe | 15.50 | Silty clay and silt to silty sand | 2007 | | | Open-ended |
| 27 | 39 | 2 | HP 310 × 110 | 25.50 | Silty sand; layered clay and silt | 1279 | 733 | 546 | |
| 28 | 39 | 3 | 324 OD Pipe | 25.40 | Silty sand; layered clay and silt | 1152 | 525 | 627 | 343 mm ∅ shoe |
| 29 | 40 | 2 | HP 310 × 110 | 24.50 | Layered sand and silty clay | 1205 | 625 | 580 | |
| 30 | 40 | 3 | 324 OD Pipe | 17.20 | Sandy silt to sand | 1128 | 544 | 584 | 343 mm ∅ shoe |
| 31 | 41 | 2 | HP 310 × 110 | 19.50 | Sand | | 1073 | | |
| 32 | 41 | 3 | 324 OD Pipe | 16.00 | Sand | | 699 | | 343 mm ∅ shoe |

[a]Steel H pile designations are size (mm) by weight (kg/m). Steel pipe piles were filled with concrete before testing, and OD is the outside diameter (mm)

[b]Embedment Length

[c]The dominating soil type, and classifications are according to MTO standards

samples, and the top and bottom of the box respectively show the first and third quartile. The line that divides the box is the median, and the whiskers show the minimum and maximum N-values. Soils above the groundwater table were excluded from the figure to reduce the influence of soil density and degree of saturation. According to the MTO soil classification system (Ministry of Transportation and Communications, 1980), the soil types were classified as clays, cohesionless silts and sands, and gravels by the dominate soil content. The gravel content was classified as none, trace, some, and gravelly/gravels according to its contents of 0%, 1–10%, 11–20%, and > 20%, respectively. Gravels can be displaced easily during testing in weak or loose soils with low confinements. Figure 3 shows the impact of confinement on SPT N-values under effective stress conditions below or above 150 kPa. The N-value generally

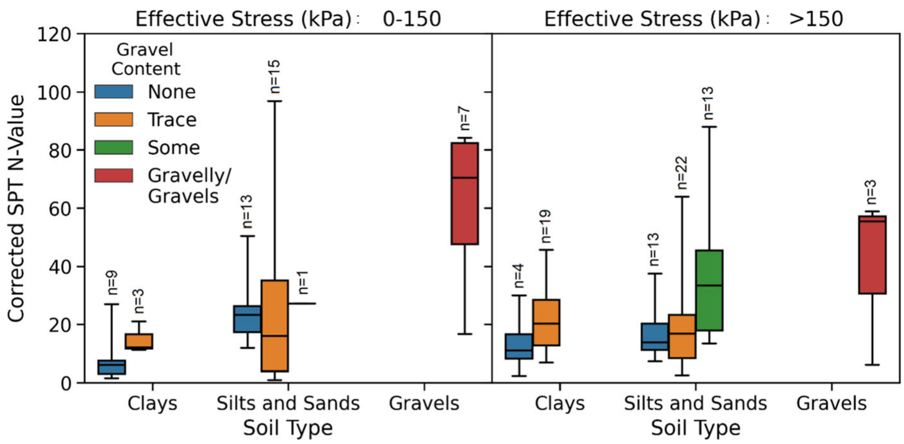


**Fig. 3** Variability of corrected SPT N-value with gravel content

increases with a higher gravel content, but this trend can experience a lot of variabilities. The SPT sampler is less likely to miss gravels and receive higher N-values in soils with high gravel contents or gravels with larger diameters. With a high and erratic N-value, the soil may appear stronger than it actually is, and this misinterpretation of the strength can lead to an over - prediction of the pile resistances. For silts and sands with an effective stress above 150 kPa, the average $N_{corr}$ was 18, 19, and 36 for none, trace, and some gravel contents, respectively. The standard deviation of $N_{corr}$ was 9.9 for gravel-free silts and sands but was 21.5 for silts and sands with some gravels. For the same effective stress category, gravels had the highest average $N_{corr}$ of 40 and the greatest standard deviation of 29.5. Although the measured N-value may also vary due to the initial void ratio and disturbance by the drilling technique, the gravel content contributes to challenges of properly characterizing glacial deposits. The difference in $N_{corr}$ and its range is significant between gravel-free soils and soils with high gravel contents.

## 4 Performance of Existing Design Methods and the Proposed Method

### 4.1 Existing Pile Design Methods Using SPT N-Values

The SPT is one of the oldest and roughest field exploration techniques in geotechnical engineering. Currently, more advanced design methods tend to use other more reliable and consistent testing methods, like cone penetration tests (Jardine et al. 2005). However, SPT is still the most popular, in many cases the only, field testing method available in the stiff or dense and gravel or boulder-rich glacial deposits. In summary, the SPT-based design methods still play a significant role in current practice. There is a need to evaluate the performance of the existing SPT-based design methods in glacial deposits. The predicted capacity ($Qu_p$) was calculated with the common $\alpha$ and $\beta$ methods for assessing their performances with the measured capacities. The existing methods were selected based on the pile types and dimensions similar to the ones used in this study. The $\beta$ method proposed by Nordlund (1963, 1979) is a semi-empirical method that was based on field tests on piles driven 7 m to 24 m into cohesionless soils. This popular method (AbdelSalam et al. 2012) was used in this study since it can account for different pile geometries, including pipe and H piles with section widths varying from 250 to 400 mm. Tomlinson studied timber, steel, and concrete piles with pile widths varying from 150 to 400 mm and pile lengths from 4 to 36 m. The Tomlinson approach is very similar to the $\alpha$ method adopted by the Canadian Foundation Engineering Manual (CFEM) (CGS 2006). The API design method was mainly developed for large diameter pipe piles but is suggested by Hannigan et al. (2016) for layered soils.

For the Nordlund method, the $q_s$ and $q_p$ were calculated following suggestions by the Federal Highway Administration (FHWA) (Hannigan et al. 2016) as follows:

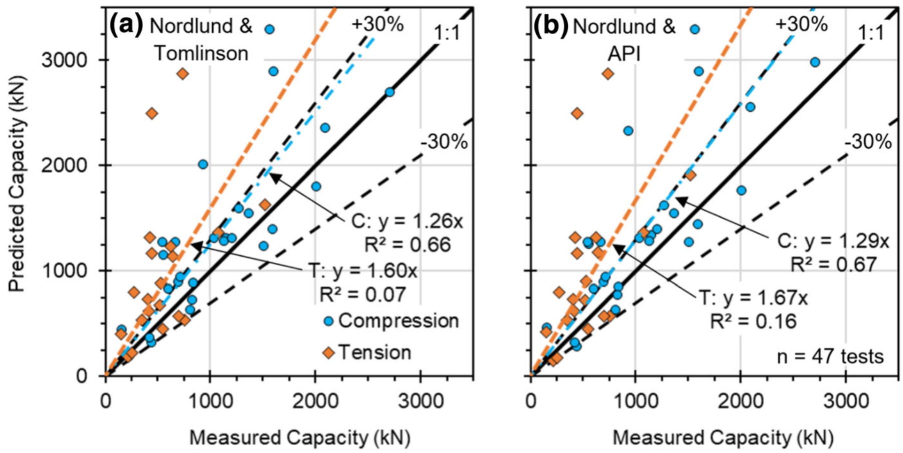


**Fig. 4** Comparison of predicted and measured capacity by the existing methods

$$q_s = K_\delta C_F \sigma' \sin\delta \tag{11}$$

$$q_p = \alpha_t N_q \sigma_t' \tag{12}$$

where $\delta$ is the soil-pile interface friction angle; $K_\delta$ is the coefficient of lateral earth pressure; $C_F$ is an empirical correction factor for when $\delta$ is not equal to $\phi'$; $\phi'$ is the soil friction angle; and $\alpha_t$ is an end bearing correction factor for consideration of the pile slenderness ratio. For $q_p$, the value of $\sigma_t'$ at the pile base was limited to 150 kPa as suggested by Hannigan et al. (2016).

For cohesive soils, both $\alpha$ methods proposed by Tomlinson (1957) and adopted by API (2000) were applied in this study. The unit resistances were determined by Eqs. (4) and (5) with the $\alpha$ methods. Since laboratory shear strength tests were not available in many cases mainly due to sampling difficulties, the shear strength parameters were obtained empirically with SPT N-values in this study. For cohesionless soils, $\phi'$ was determined by the correlation from Wolff (1989):

$$\phi' = 27.1 + 0.3N_{60} - 0.00054N_{60}^2 \tag{13}$$

For the sites with cohesive soils, $Cu$ was usually measured with UU triaxial and/or UCS tests, and the following empirical relationships by Sivirkaya and Toğrol (2006) were sufficient to determine $C_u$. $Cu$ was equal to 4 $N_{60}$ for clays, 3.8$N_{60}$ for silty clays, 3$N_{60}$ for clayey silts, and 9$N_{60}$ for desiccated (hard) clays.

For the calculations, SPT N-values were limited to a maximum of 50 for the corrected values, and H piles were assumed to be fully plugged as suggested by Hannigan et al. (2016). The predictions are compared to the measured results, as shown in Fig. 4. The lower and upper dashed lines indicate an underprediction or overprediction of the measured capacity by 30%, respectively. In the labels, "T" is for tension tests, and "C" is for compression tests.

The performance of the existing methods indicates a new method for glacial deposits is needed as they usually overpredict the capacity. Glacial deposits encountered in this study are much stronger than the soils for developing these methods. The Nordlund method (1963, 1979) and the Tomlinson (1957) method has an average $Qu_p/Qu_m$ of 1.61 with a COV of 57.9%. The combination of the Nordlund (1963, 1979) method and API (2000) method overpredict slightly more by an average factor of 1.63 with a COV of 58.2%. The inconsistency of these methods is similar to the results by Briaud and Tucker (1988) when they studied the SPT-based approach proposed by Meyerhof (1956, 1976). Since the two $\alpha$ methods provide a similar average and COV for $Qu_p/Qu_m$, the performance of the existing methods will be from the combination of Nordlund (1963, 1979) and Tomlinson (1957) methods.

Most of the variabilities by the existing design methods are due to the difficulties in accurately characterizing the shear strength parameters, namely $Cu$ and $\phi'$. Many of the cohesionless soils were classified as dense ($30 \le N_f \le 50$) to very dense ($N_f > 50$). For example, $N_f$ ranged from 38 to 154 at Site 38. In addition, the gravel content found in some of the soil profiles led to very high and erratic

N-values that were over 100. In this study, the N values were capped to a limit of 50 for determining the shear strength of soils. For the correlation recommended by Wolff (1989), these high N-values add a challenge to determine the true strength of the soil and would correspond to much larger friction angles than expected. More studies are needed to evaluate the true shear strength of glacial deposits with high N-values instead of capping them arbitrarily.

Since the existing design methods were mostly based on solid-section piles, H piles experienced more overpredictions and higher variabilities compared to pipe piles. On average, $Qu_p$ was 76% higher than $Qu_m$ with a COV of 61.0%, while pipe piles had an average $Qu_p/Qu_m$ of 1.42 and a COV of 47.7%. Even though some H and pipe piles were installed at the same site with similar soil conditions, one reason for the difference in variability can be due to the suggested soil-pile interface frictional angle, $\delta$. The Nordlund (1963, 1979) method provides an empirical relationship to determine $\delta$ from the frictional angle of soil, $\phi'$ and displaced soil volume by the pile. The average $\delta$ value was estimated by Nordlund (1963, 1979) method to be 0.62 for pipe piles and 0.77 for H piles in this study. The lateral earth pressure will likely change between the pile types due to the displaced volume, but $\delta$ may remain the same. After Everton (1991) studied the behaviour of sand on the interface of piles with shear box tests, $\delta$ was found to be independent of the soil relative density but increased with smaller grain sizes. Overall, for these two pile types, the overpredictions and variabilities by the Nordlund (1963, 1979) method can be explained by its lack of accuracy to determine the side resistance.

## 4.2 Development of the Proposed SPT Method

As shown in Fig. 5, direct correlations between the tip resistance and corrected N-value at the pile tip, $N_{pcor}$, depend on the gradation of the soil. It is found that the correlation by Meyerhof (1976) for sandy soils would be the upper bound for $q_p$, and the formula by Decourt (1995) for clays would be the lower bound. Since most of the studied sites were abundant with silts, a $K$ coefficient of 170 for cohesive soils, which includes silty clays and clayey silts, would be very similar to the coefficient of 165 for silty clays by Decourt (1995).

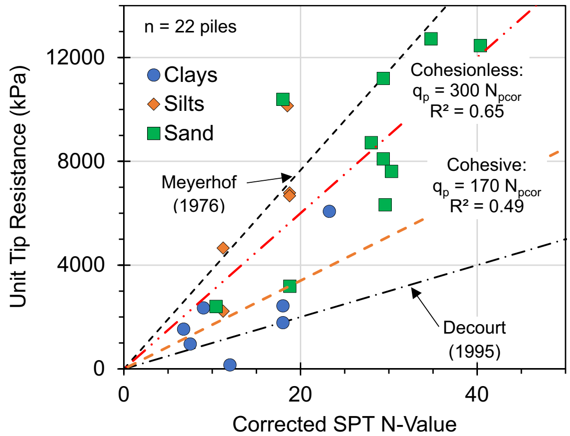


**Fig. 5** Relationship between unit tip resistance and SPT N-Values

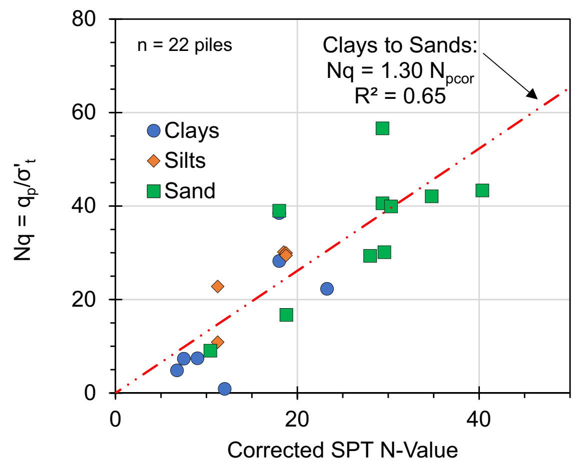


**Fig. 6** Relationship between end bearing factor and SPT N-Values

Based on the effective stress approach for cohesive and cohesionless soils, $N_q$ can be back-calculated from the vertical effective stress at the pile tip, $\sigma_t'$ and measured $q_p$, as shown for Fig. 6. The following expression proposed for $q_p$ has a coefficient of determination ($R^2$) of 0.65, which indicates a moderately strong correlation:

$$q_p[kPa] = 1.30N_{pcor}\sigma_t' \quad (14)$$

Inconsistencies still exist due to the difference in load transfer between short and long piles (Fellenius, 2019; Nordlund, 1979) and since the soil resistance depends on the soil gradation and initial void ratio. The inclusion of gravels can also increase the expected N-value, and traces of gravels were commonly found in the cohesionless soil profiles, especially closer to bedrock. Also, for cohesive soils, SPT measurements are dependent on the plasticity and stress history of the soil.

The heterogeneous site conditions provide a challenge to correlate the side resistance to the N-values along a pile. Since side resistance depends highly on the soil type and contents, the average conditions would lead to a lot of variabilities. In order to conduct a correlation, the piles were first divided into segments to consider the changing soil types and strengths. The segment lengths were as short as 30 cm and varied depending on the variability of the soil conditions. The $Qs$ was equal to the summation of the side resistances from each pile segment:

$$Qs = \sum_{i=0}^{T} A_i \cdot \overline{N_i} \cdot \sigma_i' \cdot P \cdot L_i \tag{15}$$

where $i$ is the $ith$ soil element in a soil type with a total of $T$ elements encountered along the pile length; $A_i$ is a scalar coefficient; $\overline{N}$ is the average SPT N-value along the pile length in the $ith$ soil element; $P$ is the pile perimeter; $Li$ is the thickness of the $ith$ soil element. Based mostly on the primary and secondary dominating soil contents, cohesive soils were grouped (for $i$) into desiccated (hard) clays, clays, silty clays, and clayey silts. Based on the results from Fig. 3, the side resistance will vary if the soil has high or low gravel contents. Thus, the cohesionless soils (for $i$) were categorized by the gravel content: low (trace or none); some; and high (gravelly to gravels). The scalar coefficients, $Ai$, in Eq. (15) were determined based on the criteria of obtaining the lowest mean absolute error (MAE) between the measured and predicted $Qs$. A similar approach was applied by many researchers (Aoki and Velloso 1975; Kolk and Van der Velde 1996; Van Dijk and Kolk 2011). The analysis was separated for pipe and H piles to consider the difference between their geometries.

For pipe piles, the following equations were proposed using either uncorrected or corrected N-values:

$$q_s[kPa] = \begin{cases} 13.2N_{cor}\left(\frac{\sigma'}{P_a}\right) \\ 5.66N_{cor}\left(\frac{\sigma'}{P_a}\right) \\ 5.09N_{cor}\left(\frac{\sigma'}{P_a}\right) \\ 2.25N_{cor}\left(\frac{\sigma'}{P_a}\right) \\ 2.22N_{cor}\left(\frac{\sigma'}{P_a}\right) \\ 1.12N_{cor}\left(\frac{\sigma'}{P_a}\right) \\ 1.01N_{cor}\left(\frac{\sigma'}{P_a}\right) \end{cases}$$

$$or \begin{cases} 7.40N_f\left(\frac{\sigma'}{P_a}\right), & \text{if desiccated clay} \\ 2.82N_f\left(\frac{\sigma'}{P_a}\right), & \text{if clay} \\ 2.70N_f\left(\frac{\sigma'}{P_a}\right), & \text{if silty clay} \\ 1.40N_f\left(\frac{\sigma'}{P_a}\right), & \text{if clayey silt} \\ 1.35N_f\left(\frac{\sigma'}{P_a}\right), & \text{if cohesionless with traces of gravel} \\ 1.13N_f\left(\frac{\sigma'}{P_a}\right), & \text{if cohesionless with some gravel} \\ 1.05N_f\left(\frac{\sigma'}{P_a}\right), & \text{if gravel or gravelly cohesionless} \end{cases} \tag{16}$$

For fully plugged H piles, the following equations were proposed:

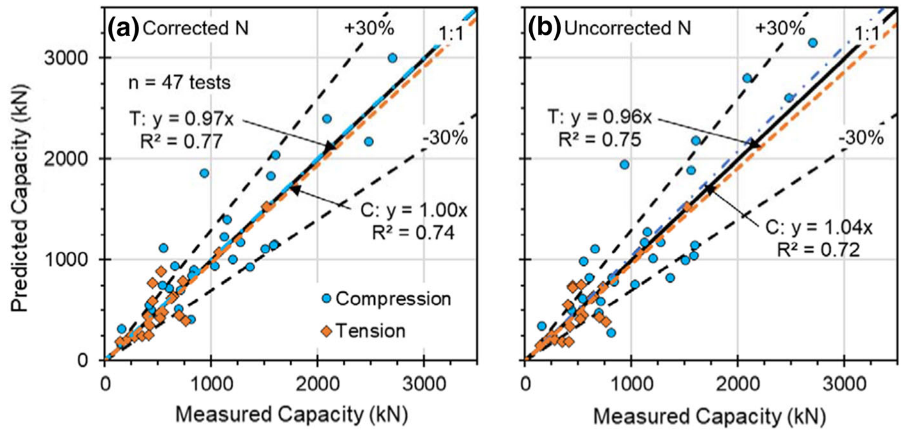


**Fig. 7** Comparison of predicted and measured capacity by the proposed method

$$q_s[kPa] = \begin{cases} 12.5N_{cor}\left(\frac{\sigma'}{P_a}\right) \\ 3.26N_{cor}\left(\frac{\sigma'}{P_a}\right) \\ 2.76N_{cor}\left(\frac{\sigma'}{P_a}\right) \\ 1.86N_{cor}\left(\frac{\sigma'}{P_a}\right) \\ 1.37N_{cor}\left(\frac{\sigma'}{P_a}\right) \\ 0.41N_{cor}\left(\frac{\sigma'}{P_a}\right) \\ 0.38N_{cor}\left(\frac{\sigma'}{P_a}\right) \end{cases}$$

$$or \begin{cases} 7.02N_f\left(\frac{\sigma'}{P_a}\right), & \text{if desiccated clay} \\ 2.68N_f\left(\frac{\sigma'}{P_a}\right), & \text{if clay} \\ 2.10N_f\left(\frac{\sigma'}{P_a}\right), & \text{if silty clay} \\ 1.40N_f\left(\frac{\sigma'}{P_a}\right), & \text{if clayey silt} \\ 0.80N_f\left(\frac{\sigma'}{P_a}\right), & \text{if cohesionless with traces of gravel} \\ 0.22N_f\left(\frac{\sigma'}{P_a}\right), & \text{if cohesionless with some gravel} \\ 0.19N_f\left(\frac{\sigma'}{P_a}\right), & \text{if gravel or gravelly cohesionless} \end{cases} \quad (17)$$

where $P_a$ is the atmospheric air pressure (= 100 kPa), $N_f$ is the uncorrected SPT blow count, $N_{cor}$ is the SPT blow count corrected for 60% hammer energy ratio.

The predicted and measured capacities from the proposed method are shown in Fig. 7. The proposed design method has unbiased predictions with an average $Qu_p/Qu_m$ of 1.06 compared to existing methods, which overpredicted by a factor of 1.61 on average. The COV is 37.1% for pipe piles and 24.8% for H piles. On the pipe piles, the over-sized base plate may create this variability as gaps may form between the pile and the soil or the lateral confinement experiences additional disturbance during driving. In general, variability also exists due to the reliability of the SPT measurements and factors related to the pile length, such as the residual loads and load transfer along piles of different lengths (Fellenius 2019; Nordlund 1963; Semple and Rigden 1986). The uncorrected N-values provide reasonable predictions with an average $Qu_p/Qu_m$ of 1.04, but the predictions are slight less consistent with a COV of 37.8% compared to using corrected N-values. Due to the high impact of the effective stress on cohesionless soils, uncorrected N-values are not recommended and are provided here only as a comparison. Depending on the content and size of gravels, the true gravel content may not be accurately detected by the SPT sampler. Thus, Eqs. (16) and (17) can be treated for the average conditions. Lower coefficients may be used if the soil is dense with high gravel contents, while higher coefficients may be applied to soils with a low gravel content.

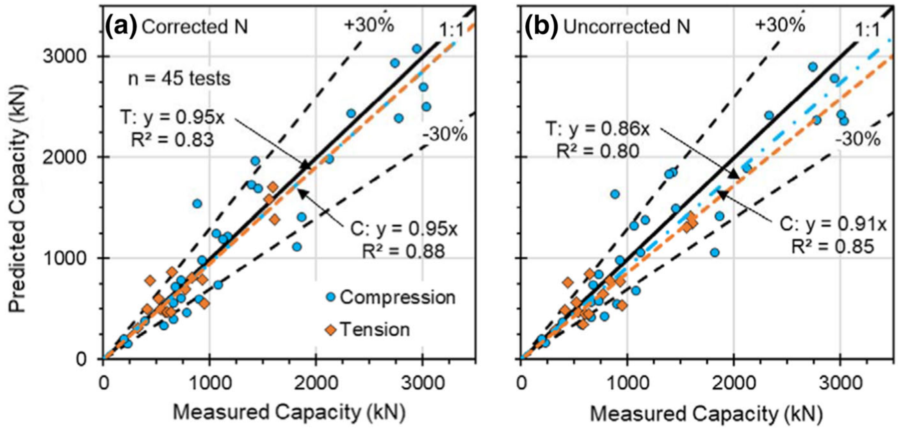


**Fig. 8** Comparison of predicted and measured capacity by the proposed method with validation pile tests

Since the new design method was developed with a limited number of cases, it is recommended to limit the values of $q_s$ and $q_p$, like Meyerhof (1976) and Decourt (1982). In general, unless local tests have been conducted, $q_s$ should not be greater than 150 kPa. The $q_p$ for cohesive and cohesionless soils can be limited to 6.35 MPa and 13 MPa, respectively. It may also be appropriate to cap the SPT N-values to 50 to ensure safe estimates.

## 5 Validation of the Proposed Method with Piles from Other Sources

The proposed design method was validated with an independent database of pile tests collected from literature. A total of 40 driven steel piles (29 H piles and 11 closed-ended pipe piles) with 45 pile load tests (29 compression and 16 tension) were collected from thirteen different sites located within the North America. All these sites were influenced by glacial activities. Soil types ranged from soft clays to dense gravelly sands. A wide range of pile dimensions were covered in these cases, with the pile width varying from 246 to 533 mm and the length from approximately 6 to 35 m. These piles were subjected to a variety of static load testing procedures, but slow maintained and quick load tests were the most common. Their failure loads were identified from their load–displacement responses according to the De Beer method.

The SPT measurements and soil classifications along the pile lengths were collected and processed before applying into Eqs. 16 and 17 to obtain the predicted pile capacities. The comparison between the measured and predicted capacities is shown in Fig. 8. Even with different piles from different sites, the proposed method provided unbiased predictions with the average $Qu_p/Qu_m$ of 0.94 for compression piles and 1.00 for tension piles. The variability is also low with a COV of 27.3% and 26.8% for compression and tension tests, respectively. More details about the pile, soil, and load test data, ratio between predicted capacity and measured capacity, $Q_{up}/Q_{um}$, can be found in Table 4.

## 6 Conclusions and Discussions

A new SPT-based design method is proposed to predict the axial capacity of driven piles in glacial deposits. The new method applies a more detailed soil classification to address the unsorted grain distributions and gravel content in glacial deposits. Based on a total of 53 full-scale static load tests conducted on driven piles in glacial deposits in the province of Ontario, Canada, the new method has an unbiased prediction with a reduced variation. After comparing the existing indirect methods suggested by Nordlund (1963, 1979), Tomlinson (1957), and API (2000), the proposed method reduces the variability by almost 50% and helps to prevent overestimations for the pile resistance in soils with a moderate gravel content. Also, for cohesionless soils, the proposed method considers the effective stress, which affects the soil

**Table 4** Summary of external sources from the literature on steel driven piles

| Case no | References | Location | Pile no | Pile type[a] | Length[b] (m) | Embedded soil type[c] | $Qu_m$ (kN) | | Test Type[e] | $Qu_p/Qu_m$ | |
|---|---|---|---|---|---|---|---|---|---|---|---|
| | | | | | | | C[d] | T[d] | | C[d] | T[d] |
| 1 | Bica et al. (2012) | Jasper County, IN, US | MCEP | 356 OD | 18.50 | Clay to silt | 1459 | | SM | 1.16 | |
| 2 | | | MHP | HP 310 × 110 | 18.50 | Clay to silt | 1867 | | SM | 0.75 | |
| 3 | Briaud and Tucker (1989) | Lock and Dam 26, Alton, IL, US | 1–2 | HP 360 × 109 | 16.46 | Sandy till | | 928 | SM | | 0.85 |
| 4 | | | 1-3A | HP 360 × 109 | 16.46 | Sandy till | 2335 | | SM | 1.04 | |
| 5 | | | 1-3B | HP 360 × 109 | 16.46 | Sandy till | | 442 | SM | | 1.76 |
| 6 | | | 1–5 | HP 360 × 109 | 18.44 | Sandy till | | 644 | Q | | 1.34 |
| 7 | | | 1–6 | HP 360 × 109 | 16.15 | Sandy till | 2777 | | Q | 0.86 | |
| 8 | | | 2–1 | HP 360 × 109 | 16.76 | Sandy till | | 832 | Q | | 0.96 |
| 9 | | | 2–8 | HP 360 × 109 | 12.19 | Sandy till | | 412 | SM | | 1.21 |
| 10 | | | 3–1 | 304 OD | 14.23 | Sandy till | 1062 | | SM | 1.17 | |
| 11 | | | 3–2 | 304 OD | 10.97 | Sandy till | | 534 | SM | | 0.94 |
| 12 | | | 3–4 | 355 OD | 14.39 | Sandy till | 882 | | SM | 1.74 | |
| 13 | | | 3–5 | 355 OD | 11.13 | Sandy till | | 517 | SM | | 1.17 |
| 14 | | | 3–7 | 406 OD | 14.57 | Sandy till | 1391 | | SM | 1.24 | |
| 15 | | | 3–8 | 406 OD | 11.13 | Sandy till | | 770 | SM | | 0.90 |
| 16 | | | 3–14 | HP 360 × 109 | 11.89 | Sandy till | | 950 | Q | | 0.58 |
| 17 | | | 3–15 | HP 360 × 109 | 11.28 | Sandy till | | 600 | Q | | 0.79 |
| 18 | | | 3–16 | HP 360 × 109 | 11.28 | Sandy till | | 640 | Q | | 0.74 |
| 19 | Davis (2012) | Sakonnet River, RI, US | HA-HP | H 360 × 174 | 34.60 | Sand and silt | 2131 | | Q | 0.93 | |
| 20 | Goble et al. (1972) | West Lafayette, IN, US | Test1 | HP 250 × 85 | 15.24 | Sand to gravelly sand | 737 | 320 | CRP | 0.81 | 0.98 |
| 21 | Mansur et al. (1958) | Old River, LA, US | 1 | HP 360 × 109 | 24.69 | Silt to sand | 3040 | | SC | 0.82 | |
| 22 | | | 2 | 533 OD | 19.81 | Silt to sand | 2750 | 1606 | SC | 1.07 | 0.86 |
| 23 | | | 3 | HP 360 × 109 | 21.64 | Silt to sand | 1432 | | SC | 1.38 | |
| 24 | | | 4 | 431 OD | 20.12 | Silt to sand | 3014 | 1558 | SC | 0.89 | 1.02 |
| 25 | | | 5 | 431 OD | 13.72 | Silt | 1129 | 580 | SC | 1.05 | 0.81 |
| 26 | | | 6 | 482 OD | 19.81 | Silt to sand | 2949 | 1594 | SC | 1.04 | 1.07 |
| 27 | Ng et al. (2011) | Mills County, IA, US | ISU2 | HP 250 × 63 | 17.02 | Clay to silty clay | 573 | | Q | 0.57 | |
| 28 | | Polk County, IA, US | ISU3 | HP 250 × 63 | 15.54 | Clayey silt | 666 | | Q | 0.60 | |
| 29 | | Jasper County, IA, US | ISU4 | HP 250 × 63 | 17.31 | Clay and clayey silt | 684 | | Q | 1.04 | |
| 30 | | Clarke County, IA, US | ISU5 | HP 250 × 63 | 17.27 | Clay | 1171 | | Q | 1.04 | |
| 31 | | Buchanan County, IA, US | ISU6 | HP 250 × 63 | 17.43 | Clay to clayey silt | 932 | | Q | 1.05 | |
| 32 | | | ISU7 | HP 250 × 63 | 8.20 | Clay and sand | 234 | | Q | 0.65 | |
| 33 | | Poweshiek County, IA, US | ISU8 | HP 250 × 63 | 17.44 | Clay to silty clay | 730 | | Q | 1.07 | |
| 34 | | Des Moines County, IA, US | ISU9 | HP 250 × 63 | 15.09 | Clay and sand | 665 | | Q | 0.84 | |
| 35 | Tavenas (1970) | St. Charles River, QC, Canada | H1 | HP 310 × 110 | 5.73 | Granular fill | 200 | | CTI | 0.98 | |
| 36 | | | H2 | HP 310 × 110 | 8.73 | Granular fill and sand | 395 | | CTI | 0.96 | |
| 37 | | | H3 | HP 310 × 110 | 11.73 | Granular fill and sand | 784 | | CTI | 0.59 | |
| 38 | | | H4 | HP 310 × 110 | 14.73 | Sand | 902 | | CTI | 0.66 | |

**Table 4** continued

| Case no | References | Location | Pile no | Pile type[a] | Length[b] (m) | Embedded soil type[c] | $Qu_m$ (kN) | | Test Type[e] | $Qu_p/Qu_m$ | |
|---|---|---|---|---|---|---|---|---|---|---|---|
| | | | | | | | C[d] | T[d] | | C[d] | T[d] |
| 39 | | | H5 | HP 310 × 110 | 17.73 | Sand | 1080 | | CTI | 0.68 | |
| 40 | | | H6 | HP 310 × 110 | 20.73 | Sand | 1822 | | CTI | 0.61 | |

[a]Steel H pile designations are size (mm) by weight (kg/m). For steel pipe piles, OD is the outside diameter (mm)

[b]Embedment Length

[c]The dominating soil type, and classifications are according to MTO standards

[d]*C* compression and *T* tension

[e]*CRP* constant rate of penetration, *CTI* constant time interval, *Q* quick, *SC* static cyclic, and *SM* slow maintained

lateral confinement and pile resistances, but direct design methods are commonly stress independent.

A few improvements can increase the reliability of the proposed and existing design methods:

(1) The information in this study was limited to the load and deformation measurements at the top of the piles. The side resistance will likely be lower during a tension test compared to a compression test. The tip resistance may be overestimated by the suggested method. The results from fully instrumented piles can help to isolate the difference in loading direction.
(2) This study identified the capacity with the De Beer failure criterion, but other failure criteria may slightly change the magnitude of the capacity and the interaction between pile side and tip resistances.

**Acknowledgements** This study was made possible with funding initially from the National Sciences and Engineering Research Council of Canada with an Engage program and kindly supported by Arup Canada Inc. and then funded continuously by the Ministry of Transportation of Ontario with the Highways Infrastructure Innovations Funding Program. The authors also acknowledge the Canada Graduate Scholarship-Master's Award received by the first author. The authors would like to thank Mr. David Staseff and Ms. Minkyung Kwak from MTO for sharing the database of pile load tests and Ms. Mei Cheong and Mr. Colin McCreath from Arup Canada Inc. for sharing their experience and comments towards this research.

## References

AbdelSalam SS, Sritharan S, Suleiman MT, Roling M (2012) Development of LRFD procedures for bridge pile foundations in Iowa. Vol. III: Recommended resistance factors with consideration of construction control and setup (Report No. IHRB: Project TR-584). Ames, IA: Iowa Department of Transportation

Alkroosh I, Nikraz H (2014) Predicting pile dynamic capacity via application of an evolutionary algorithm. Soils Found 54(2):233–242

American Petroleum Institute (API) (2000) Recommended practice for planning, designing, and constructing fixed offshore platforms-working stress design: API Recommended Practice 2A-WSD (RP 2A-WSD), 21st edn. API, Washington, DC

Aoki N, Velloso DA (1975) An approximate method to estimate the bearing capacity of piles. In: Proceedings of the fifth Pan-American conference on soil mechanics and foundation engineering, Buenos Aires, Argentina, pp 367–376

Barnett PJ (1992) Chapter 21: quaternary geology of Ontario. In: Thurston PC, Williams HR, Sutcliffe RH, Scott GM (eds) Geology of Ontario: Ontario geological survey. Ontario Ministry of Northern Development and Mines, Sudbury, pp 1011–1088

Benali A, Boukhatem B, Hussien MN, Nechnech A, Karray M (2017) Prediction of axial capacity of piles driven in non-cohesive soils based on neural networks approach. J Civ Eng Manag 23(23):393–408

Bica AVD, Prezzi M, Seo H, Salgado R, Kim D (2014). Instrumentation and axial load testing of displacement piles. In: Proceedings of the institution of civil engineers – geotechnical engineering167: 238–252

Boonstra GC (1936) Pile loading tests at Zwijndrecht, Holland. In: Proceedings of the 1st international conference on soil mechanics and foundation engineering, Cambridge, MA, 1, pp 185–191

Briaud J, Tucker LM (1988) Measured and predicted axial response of 98 piles. J Geotech Eng, ASCE 114(9):984–1001

Briaud J, Moore BH, Mitchell GB (1989) Analysis of pile load tests at Lock and Dam 26. In: Kulhawy FH (ed) Foundation engineering: current principles and practices. ASCE, Reston, pp 925–942

Brown RP (2001) Predicting the ultimate axial resistance of single driven piles (Doctoral dissertation). Department of Civil Engineering, University of Texas, Austin, TX

Burland JB (1973) Shaft friction of piles in clay–a simple fundamental approach. Ground Eng 6(3):30–42

Canadian Geotechnical Society (CGS) (2006) Canadian foundation engineering manual, 4th edn. CGS, Richmond

Davis S (2012) Accuracy of static capacity method and calibration of resistance factors for driven piles in Rhode Island soils [Master's thesis, University of Rhode Island]

De Beer EE (1967) Proefondervindelijke bijdrage tot de studie van het grensdraagvermogen van zand onder funderingen op staal (Deel 1). Annales des travaux publics de Belgique (2nd series) 68(6):481–504

De Beer EE (1968). Proefondervindelijke bijdrage tot de studie van het grensdraagvermogen van zand onder funderingen op staal (Deel 2–3). Annales des travaux publics de Belgique (2nd series), 69(1):44–88; *69*(4), 321–360

Decourt L (1995) Prediction of load-settlement relationships for foundations on the basis of the SPT-T. Ciclo De Conferencias Internationale, Mexico City, Mexico 1:85–104

Decourt L (1982) Predictions of bearing capacity based exclusively on N values of the SPT. In: Proceedings of the 2nd European symposium on penetration testing, Amsterdam, vol 1, pp 29–34

Everton S (1991) Behaviour of sands in shear box interface tests (MSc Thesis). University of Imperial College, London, UK

Fellenius BH (1980) The analysis of results from routine pile load tests. Ground Eng 13(6):19–31

Fellenius BH (2019) Basics of foundation design. Pile Buck International Inc, Vero Beach

Goble GG, Kovacs WD, Rausche F (1972) Field demonstration: response of instrumented piles to driving and load testing. In: Proceedings of the specialty conference on performance of earth and earth-supported structures, lafayette, IN, pp. 3–38

Golafzani SH, Eslami A, Chenari RJ (2020) Probabilistic assessment of model uncertainty for prediction of pile foundation bearing capacity; static analysis, SPT and CPT-based methods. Geotech Geol Eng 38:5023–5041

Hannigan PJ, Rausche F, Likins GE, Robinson BR, Becker ML (2016) Geotechnical engineering circular No. 12 – Volume I: design and construction of driven pile foundations (Publication No. FHWA-NHI-16–009). Washington, DC: Federal Highway Administration (FHWA)

Jardine R, Chow F, Overy R, Standing J (2005) ICP design methods for driven piles in sands and clays. Thomas Telford Publishing, London

Kolk HJ, Van der Velde E (1996) A reliable method to determine friction capacity of pile driven into clays. In: Proceedings of the 28th offshore technology conference, pp 337–346

Kulhawy FH, Mayne PW (1990) Manual on estimating soil properties for foundation design: Report EL-6800. Electric Power Research Institute, Palo Alto

Legget RF (ed) (1965) Soils in Canada: Geological, Pedological, and Engineering Studies. The Royal Society of Canada, Toronto

Mansur CI, Kaufman RI (1958) Pile tests, Low-sill Structure, Old River, Louisiana. J Soil Mech Found Division 82(4):1–33

Martin RE, Seli JJ, Powell GW, Bertoulin M (1987) Concrete pile design in tidewater, Virginia. J Geotech Eng, ASCE 113(6):568–585

McVay MC, Birgisson B, Zhang LM, Perez A, Putcha S (2000) Load and resistance factor design (LRFD) for driven piles using dynamic methods–a Florida perspective. Geotech Test J 23(1):55–66

Meyerhof GG (1956) Penetration tests and bearing capacity of cohesionless soils. J Soil Mech Found Division, ASCE 82(1):1–19

Meyerhof GG (1976) Bearing capacity and settlement of pile foundations. J Geotech Eng Division, ASCE 102(3):197–228

Milligan V (1976) Geotechnical aspects of glacial tills. In: Legget RF (ed) Glacial till: an inter-disciplinary study. The Royal Society of Canada, Ottawa, pp 269–291

Ministry of Transportation and Communications (MTC) (1980) MTC soil classification manual. MTC, Downsview

Ministry of Transportation of Ontario (MTO) (1993) Pile load and extraction tests: 1954–1992 (Rev. 1993). MTO, Toronto

Ng KW, Suleiman MT, Roling M, AbdelSalam SS, Sritharan S (2011) Development of LRFD design procedures for bridge piles in iowa—field testing of steel H-piles in clay, sand, and mixed soils and data analysis (Vol. II). Iowa Highway Research Board, Ames

Nordlund RL (1963) Bearing capacity of piles in cohesionless soils. J Soil Mech Found Division, ASCE 89(3):1–36

Nordlund RL (1979) Point bearing and shaft friction of piles in sand. In: Missouri-Rolla 5th Annual short course on the fundamental of deep foundation design, St. Louis, MI

Semple RM, Rigden WJ (1986) Shaft capacity of driven piles in clay. Ground Eng 19:11–19

Shariatmadari N, Eslami A, Karimpour-Fard M (2008) Bearing capacity of driven piles in sands from SPT-applied to 60 case histories. Iran J Sci Tech 32(B2):125–140

Shioi Y, Fukui J (1982) Application of N-value to design foundations in Japan. In: Proceedings of the 2nd European symposium on penetration testing, Amsterdam, vol 1, pp 159–164

Sivrikaya O, Toğrol E (2006) Determination of undrained shear strength of fine-grained soils by means of SPT and its applications in Turkey. Eng Geol 86(1):52–69

Sowers GF (1951) Modern Procedures for Underground Investigations. Proc Am Soc Civ Eng 80(435):1–11

Tang C, Phoon K-K (2018) Evaluation of model uncertainties in reliability-based design of steel H-piles in axial compression. Can Geotech J 55:1513–1532

Tavenas FA (1971) Load tests results on friction piles in sand. Can Geotech J 8:7–22

Thorburn S, MacVicar SL (1971) Pile load tests to failure in the Clyde alluvium. In: Behaviour of piles, vol 1, no 7, pp 53–54. Institution of Civil Engineers, London

Tomlinson MJ (1957) The adhesion of piles driven in clay soils. In: Proceedings of the 4th international conference of soil mechanics, vol 2, pp 66–71

Van Dijk BFK, Kolk HJ (2011) CPT-based design method for axial capacity of offshore piles in clays. Proc Front Offshore Geotech II:555–560

Wolff TF (1989). Pile capacity prediction using parameter functions. In: Predicted and observed axial behavior of piles: results of a pile prediction symposium (ASCE Geotechnical Special Publication No. 23), pp 96–106

Xiao D, Yang H (2011) Back analysis of static pile load test for SPT-based pile design: a Singapore experience. In: Proceedings of advances in pile foundations, geosynthetics, geoinvestigations, and foundation failure analysis and repairs, pp 144–152

Yagiz S, Akyol E, Sen G (2008) Relationship between the standard penetration test and pressuremeter test on sandy silty clays: a case study from Denizli. Bull Eng Geol Environ 67:405–410

Zhang L, Chen J-J (2012) Effect of spatial correlation of standard penetration test (SPT) data on bearing capacity of driven piles in sand. Can Geotech J 49:394–402